

Engineering the Thermopower of C₆₀ Molecular Junctions

Charalambos Evangelis,[†] Katalin Gillemot,[‡] Edmund Leary,^{†,§} M. Teresa González,[§] Gabino Rubio-Bollinger,^{†,||} Colin J. Lambert,^{*,‡} and Nicolás Agrait^{*,†,§,||}

[†]Departamento de Física de la Materia Condensada, Universidad Autónoma de Madrid, Madrid, Spain

[‡]Department of Physics, Lancaster University, Lancaster, United Kingdom

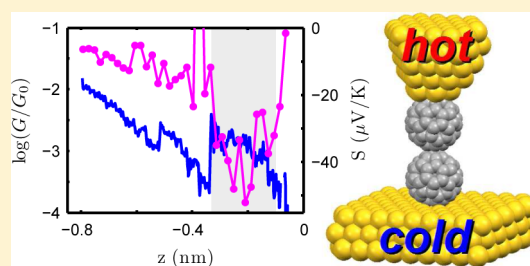
[§]Instituto Madrileño de Estudios Avanzados en Nanociencia IMDEA-Nanociencia, Madrid, Spain

^{||}Instituto Universitario de Ciencia de Materiales “Nicolás Cabrera”, Universidad Autónoma de Madrid, Madrid, Spain

Supporting Information

ABSTRACT: We report the measurement of conductance and thermopower of C₆₀ molecular junctions using a scanning tunneling microscope (STM). In contrast to previous measurements, we use the imaging capability of the STM to determine precisely the number of molecules in the junction and measure thermopower and conductance continuously and simultaneously during formation and breaking of the molecular junction, achieving a complete characterization at the single-molecule level. We find that the thermopower of C₆₀ dimers formed by trapping a C₆₀ on the tip and contacting an isolated C₆₀ almost doubles with respect to that of a single C₆₀ and is among the highest values measured to date for organic materials. Density functional theory calculations show that the thermopower and the figure of merit continue increasing with the number of C₆₀ molecules, demonstrating the enhancement of thermoelectric performance by manipulation of intermolecular interactions.

KEYWORDS: Molecular thermopower, molecular conductance, density functional theory, single molecule



The development of new higher-efficiency and low-cost thermoelectric devices is a desirable technology that would allow direct heat-to-electrical energy conversion from otherwise wasted low-level heat sources and would have an enormous impact on global energy consumption. Nanoscale systems and especially organic junctions are very promising in this respect due to the fact that transport takes place through discrete energy levels.¹ The ability to measure thermopower in single-molecule junctions opens the way to developing fundamentally new strategies for enhancing the conversion of heat into electric energy.^{2,3} Here we present detailed molecular-scale thermopower measurements and density functional calculations on C₆₀ junctions demonstrating that thermopower can be almost doubled by tuning the interaction between two neighboring C₆₀ molecules under ambient conditions and further doubled by coupling three C₆₀s. This trend is accompanied by an unprecedented increase in the thermoelectric figure of merit ZT.

The thermopower or Seebeck coefficient *S* of a material or of a nanojunction is defined as

$$S = -\frac{\Delta V}{\Delta T}$$

where ΔV is the voltage difference between the two ends of the junction when a temperature difference ΔT is established between them. The aim of this paper is to report a new strategy for increasing the thermopower at a molecular scale by tuning the intermolecular coupling between identical molecules. This

strategy differs from various intramolecular approaches to tuning *S*, which include varying the chemical composition,³ varying the position of intramolecular energy levels relative to the work function of metallic electrodes,^{4,5} systematically increasing the single-molecule lengths within a family of molecules,⁶ and systematically varying the conformation of molecules.⁷ Unlike these studies, our approach to enhancing thermopower involves varying the intermolecular coupling between chemically identical molecules. We demonstrate both experimentally and theoretically the enhancement of thermopower *S* and of the thermoelectric figure of merit ZT in molecular scale junctions and since thermopower is an intensive quantity (unlike electrical conductance) these findings point the way toward enhancing the thermoelectric properties of few-layer C₆₀ films.

Thermopower at the molecular scale can be measured using a modified scanning tunneling microscope (STM) setup. While the characterization of a junction at the molecular level requires monitoring of its conductance during formation and subsequent breaking, in most experiments reported to date conductance and thermopower are either not measured in the same junctions,^{1–4} or the thermopower is measured just at one specific point during the evolution of the junction.⁸ In

Received: February 13, 2013

Revised: March 27, 2013

Published: April 1, 2013

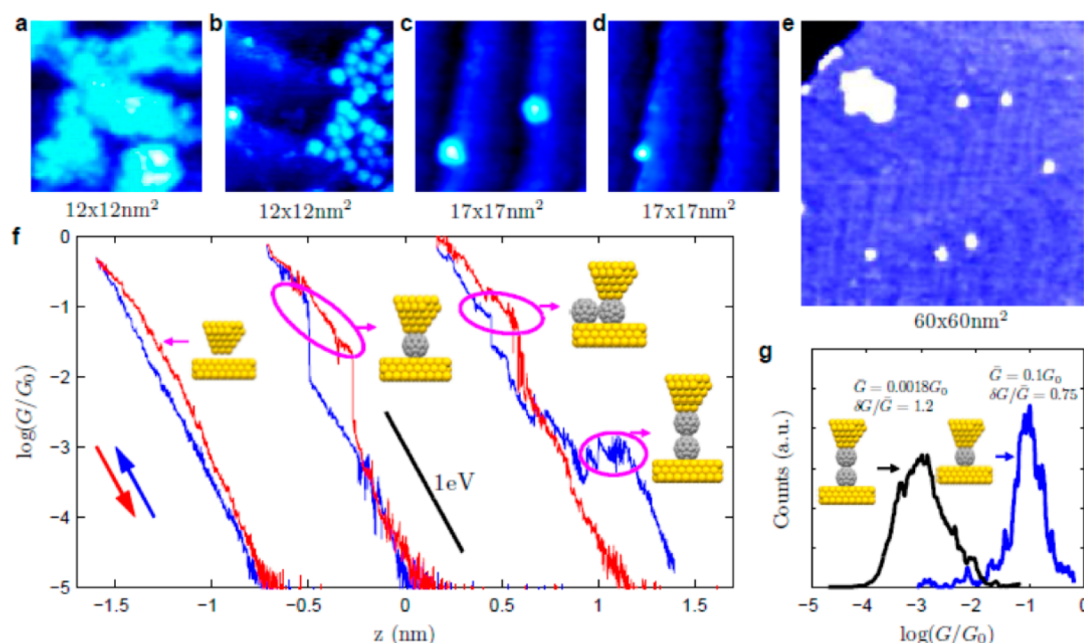


Figure 1. (a–e) STM topographic images of C_{60} molecules on Au(111). Small cluster imaged with a bare gold tip (a) and a C_{60} -tip (b), respectively. (c) Two C_{60} molecules imaged with a bare gold tip. (d) The same area shown in (c) after one of the molecules has been picked up by the tip, notice the enhanced resolution for this C_{60} -tip. (e) Large area scan showing C_{60} molecules on a terrace and at step edges. The herringbone reconstruction is observed on the terrace. (f) Approach (blue) and retraction (red) conductance curves for a bare gold tip on bare gold (leftmost traces); bare gold tip on an isolated C_{60} molecule (central traces); and C_{60} tip on an isolated C_{60} molecule (rightmost traces). The point of contact for a single C_{60} and for the C_{60} dimer are shown. The slope corresponding to an apparent tunneling barrier of 1 eV is also shown. (g) Histograms of the conductance of a bare gold tip on an isolated C_{60} molecule (blue curve) and of the conductance of a C_{60} tip on an isolated C_{60} molecule (black curve) at the points where contact is established (see Supporting Information Figures S1 and S2 for more details).

contrast to these previous experiments, we use the imaging capability of the STM to determine precisely the number of molecules in the junction and measure thermopower and conductance simultaneously during the whole evolution of the molecular junction, thereby achieving a complete characterization at the single-molecule level.

To demonstrate the enhancement of thermoelectric performance by tuning intermolecular coupling, we have chosen to investigate C_{60} molecules deposited on gold. We deposit C_{60} using the drop casting technique from solution at very low concentration and perform the experiment at ambient conditions. Small clusters and isolated molecules immobilized at monatomic steps or sometimes on the gold terraces can be observed, as shown in Figure 1. By direct contact (as described below), it is possible to attach a C_{60} molecule to the tip. The resulting C_{60} -tip yields an enhanced resolution⁹ (see Figure 1).

To form a nanojunction, we open the feedback loop of the STM and move the tip toward the sample while monitoring the conductance. In order to avoid metallic contact between tip and substrate,¹⁰ the motion is reversed when the conductance reaches a predefined threshold, $G < G_0$, where $G_0 = 2e^2/h$ is the quantum of conductance, e is the electron's charge, and h is Planck's constant. Three different types of nanojunction with characteristic conductance traces are obtained, as illustrated in Figure 1f. Approach and retraction of a bare Au-tip on a bare gold area results in a featureless conductance versus tip displacement z curve (leftmost curves in Figure 1f) corresponding to motion in the tunneling regime with an apparent tunneling barrier of about 1 eV, as typically observed in ambient conditions.¹¹ In contrast, approach and retraction of a bare gold tip on an isolated C_{60} molecule yields conductance traces with an abrupt jump or change of slope, signaling contact

with the C_{60} molecule, followed by a reduction in the slope as the molecule is pressed by the tip (central curves in Figure 1f). The fact that the retraction curve shows similar features and small hysteresis indicates that the junction is unaltered after separation. At the point where contact is established, the conductance is typically $G = 0.1 G_0$ with a relatively narrow distribution as shown in the histogram of Figure 1g (blue curve). This value is in good agreement with observed values for C_{60} between gold electrodes measured in ultrahigh vacuum (UHV) and at low temperatures^{12,13} and somewhat lower than those of C_{60} on Cu^{9,14} in UHV. Contacting a C_{60} molecule often results in the molecule being transferred to the tip. Approach and retraction of one of these C_{60} tips on the bare gold results in a conductance curve similar to that previously described for a bare gold tip on an isolated C_{60} molecule, while approach and retraction on an isolated C_{60} molecule yields a conductance curve with a characteristic shoulder indicating the formation of an Au– C_{60} – C_{60} –Au junction. The subsequent squeezing out of the junction of one of the C_{60} molecules results in a drop in conductance followed by an increase as an Au– C_{60} –Au junction forms (rightmost curves in Figure 1f). The retraction curve is similar to that of a single C_{60} (central traces in Figure 1f) indicating the effective expelling of one of the molecules from the junction. The average conductance of this C_{60} dimer is approximately $10^{-3} G_0$, as shown in the corresponding histogram in Figure 1g (black curve). The conductance of C_{60} dimers has been previously reported using Cu electrodes, and as in the case of a single C_{60} between Cu electrodes higher values are found.⁹

When a temperature difference ΔT between the tip and the substrate is established in addition to the voltage difference ΔV

(see Figure 2d and Supporting Information), the current through the junction is given by

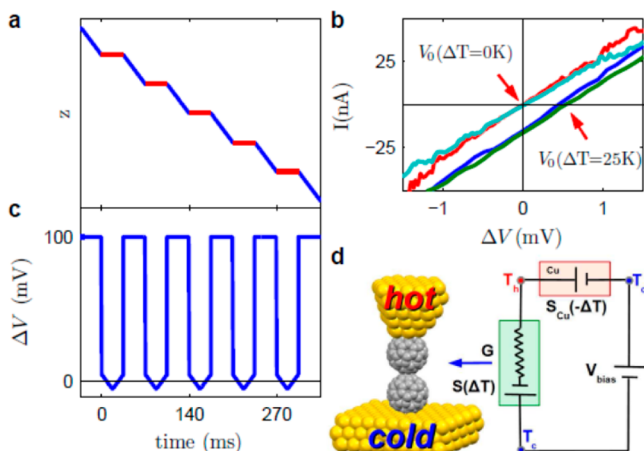


Figure 2. Technique for the simultaneous measurement of thermopower and conductance. (a,c) Tip displacement z and bias voltage applied at the molecular junction, respectively, as a function of time. The bias voltage is maintained at 100 mV during the tip motion and swept between ± 5 mV while the tip is stationary. In each approaching–separating cycle, 50–100 I – V traces are acquired. (b) Experimental I – V curves showing the voltage offset due to the temperature difference. (d) Schematic representation of the setup. The tip is heated to a temperature T_h above ambient temperature T_c , while the substrate is maintained at T_c (see Supporting Information Figure S3 for more details of the thermal circuit).

$$I = \Delta V + L\Delta T = G(V_{\text{bias}} - S_{\text{Cu}}\Delta T + S\Delta T)$$

where G is the conductance of the junction, $L = GS$ is the thermal response coefficient,^{7,15} V_{bias} is the bias voltage applied to the tip, S is the thermopower of the junction, and S_{Cu} is the thermopower of the copper wire connecting the tip ($S_{\text{Cu}} = 1.85$

$\mu\text{V/K}^4$). To measure the thermopower, we follow the same procedure for contacting the molecules described above, but now the tip motion is stopped at fixed intervals of typically 20–30 pm (see Figure 2a), while the bias voltage is swept (see Figure 2c). The corresponding current versus voltage curves, or I – V curves, show a temperature-dependent voltage offset equal to $V_0 = -(S - S_{\text{Cu}})\Delta T$. Thus, the thermopower, S , and the conductance G of the junction are measured simultaneously during approach and retraction.

We have measured the thermopower at two temperature differences $\Delta T = 12$ and 25 K for a total of 119 single C_{60} junctions (61 at $\Delta T = 12$ K and 58 at $\Delta T = 25$ K) and 23 C_{60} dimers (8 at $\Delta T = 12$ K and 15 at $\Delta T = 25$ K). In Figure 3a, we show an example of conductance and thermopower traces measured simultaneously on a single C_{60} molecule. Contact formation is clearly indicated by the abrupt jump in the conductance which results in an abrupt jump in the thermopower. Subsequent jumps in the conductance indicating rearrangements on the atomic scale¹⁰ are also reflected in jumps in the thermopower, demonstrating the sensitivity of thermopower to atomic details. For this particular single C_{60} junction, the thermopower varies in the range of -18 to -23 $\mu\text{V/K}$ presenting the largest values at contact formation. The thermopower for all the measured C_{60} junctions are in the range of -40 to 0 $\mu\text{V/K}$ with a mean value of -18 $\mu\text{V/K}$ (see Figure 4a and Supporting Information Figure S4). This is somewhat higher than the value of -14.5 $\mu\text{V/K}$ recently obtained by Yee et al.⁴ on fullerene junctions measured using the break junction technique. In Figure 3d, we show an example of conductance and thermopower traces measured simultaneously on a C_{60} dimer. The formation of the dimer is clearly identified by the already mentioned shoulder in the conductance. We can observe that a corresponding shoulder is present in the thermopower with values in the range of -25 to -50 $\mu\text{V/K}$ for this particular dimer. The maximum value that we have measured for a C_{60} dimer is -72 $\mu\text{V/K}$, and the mean

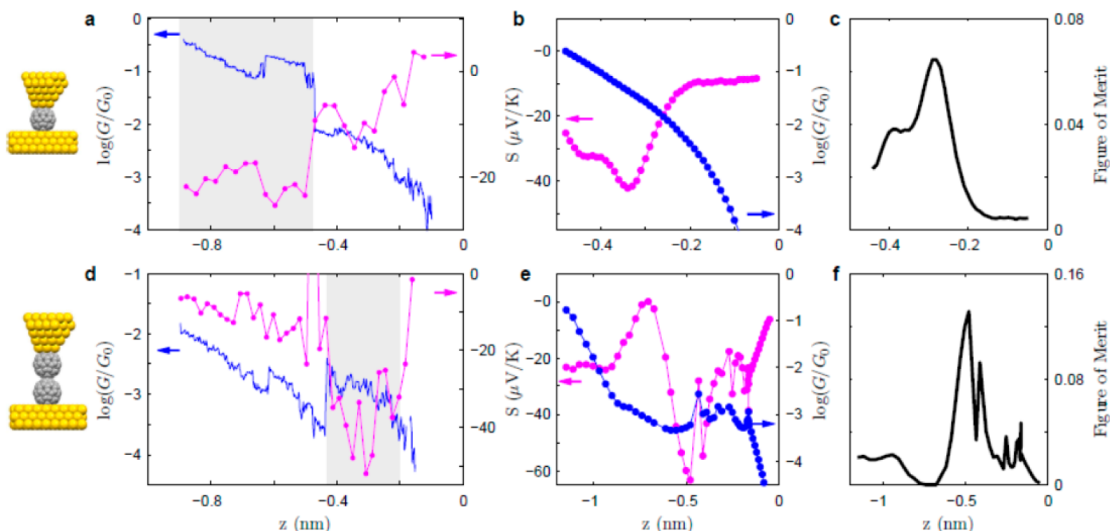


Figure 3. (a) Conductance at 100 mV (blue) and thermopower (magenta), simultaneously acquired, for approach on a single C_{60} molecule. In this measurement the temperature difference was $\Delta T = 25$ K. The shaded area indicates the range of z for which the Au– C_{60} –Au junction is already formed. (b) Theoretical conductance (blue) and thermopower versus distance for a single C_{60} . (c) Calculated figure of merit ZT for a single C_{60} . (d) Conductance at 100 mV (blue) and thermopower (magenta), simultaneously acquired, during the formation of the C_{60} dimer. In this measurement, the temperature difference was $\Delta T = 12$ K. The shaded area indicates the range in which the C_{60} dimer is in the junction. (e) Theoretical conductance (blue) and thermopower versus distance for the C_{60} dimer. (f) Calculated figure of merit ZT for a C_{60} dimer. (See Supporting Information Figure S4, for examples of approach and retraction conductance and thermopower curves on single C_{60} molecules and dimers.)

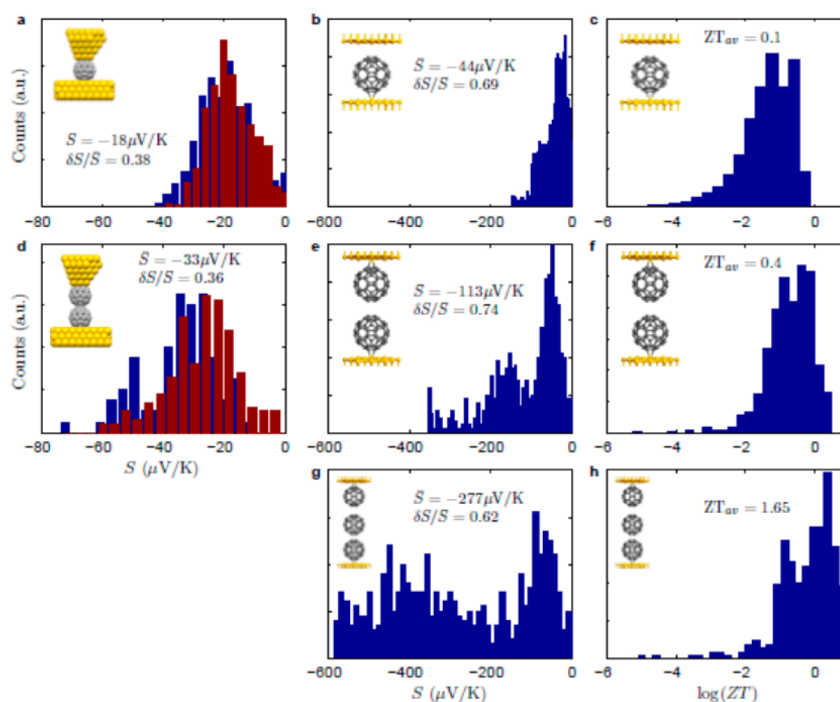


Figure 4. (a) Histogram of experimental thermopower values at contact for a single C_{60} molecule, measured at $\Delta T = 12\text{ K}$ (blue) and 25 K (red). (b,c) Histograms of the theoretically computed thermopower and figure of merit, respectively, for a single C_{60} . (d) Histogram of experimental thermopower values at contact for a C_{60} dimer, measured at $\Delta T = 12\text{ K}$ (blue) and 25 K (red). Histograms of the theoretically computed thermopower (e) and figure of merit (f), respectively, for a C_{60} dimer. Histograms of the theoretically computed thermopower (g) and figure of merit (h) for a C_{60} trimer. For further details on the generation of the histograms for the theoretically computed thermopower and figure of merit see Supporting Information. \bar{S} is the mean value of the thermopower δS is the standard deviation.

value $-33\text{ }\mu\text{V/K}$ (see Figure 4d and Supporting Information Figure S4). These values of S for the C_{60} dimer are almost double those for the single C_{60} and among the highest values measured to date for organic materials.

To analyze the underlying transport mechanisms and to extend our understanding beyond structures that are currently experimentally accessible, we have performed large-scale quantum transport calculations on single-, double- and triple- C_{60} junctions, based on density functional theory (DFT),¹⁶ using the ab initio code SMEAGOL¹⁷ which combines the Hamiltonian provided by the DFT code SIESTA¹⁸ with the nonequilibrium Green's function formalism. Further details about the above computation methods are given in the Supporting Information. Figure 3b,e shows examples of predicted conductance and thermopower curves as a function of electrode separation for a single C_{60} and a chain of two C_{60} s, respectively, and in addition Figure 3c,f shows curves of the figure of merit ZT , which are inaccessible in our experiments. These calculations reveal that both the conductance and thermopower depend only weakly on the orientation of the molecule but are sensitive to the intermolecular coupling and the positions of the frontier orbitals relative to the Fermi level, all of which fluctuate as the electrode separation is increased.

For single-, double- and triple- C_{60} junctions, Figure 4b,e,g shows the histograms from these theoretical curves across a range of electrode separations and a range of different positions for the Fermi energy (see Supporting Information for more details). Although these calculations overestimate the values for the thermopower and the conductance, they do reproduce the experimental trends and support all the main conclusions from the experiments. The main discrepancy with experiment is associated with uncertainty in the junction geometry, since the

precise atomic-scale configuration of the electrodes is not known and is likely to vary both between and along pulling curves. For the future, if tips with known geometries became available, it would be possible to further improve the calculations. In particular, we also find that the average thermopower for a chain of two C_{60} s is approximately 100% higher than that of a single C_{60} with a further doubling predicted for a chain of three C_{60} s.

From the theoretical histograms of Figure 4c,f,h, we find that the average value for ZT is also enhanced by introducing more on-the-tip C_{60} s and tuning the coupling between them. For a single C_{60} we predict the average $ZT = 0.1$, for two C_{60} s $ZT = 0.4$, while for the 3 C_{60} s $ZT = 1.65$, which represents a 4-fold and a 16-fold increase, respectively. This suggests that C_{60} films with weakly coupled layers have the potential to be competitive with the best available values for inorganic materials, although it should be noted that our predictions for ZT include only the electronic contribution to the thermal conductance, which ignores parasitic contributions from phonons and therefore represents an upper bound.

In agreement with refs 1 and 15, the relative fluctuation in the thermopower is found to be smaller than that of the conductance and furthermore this trend becomes more pronounced for multi- C_{60} junctions. For example for the triple- C_{60} s we find theoretically that $\delta S/\bar{S} = 0.62$, whereas $\delta G/\bar{G} = S$, where δS and δG are the standard deviations and \bar{S} and \bar{G} the mean values. Since the sensitivity of S to atomic-scale fluctuations is lower than that of electrical conductance, thermopower is a particularly attractive property for investigation and optimization at a molecular scale.

In summary, we have demonstrated for the first time that the thermopower and figure of merit ZT of molecular junctions can

be enhanced by manipulation of intermolecular interactions at ambient conditions. In particular, we have shown that the thermopower of a C_{60} molecule can be doubled by coupling two C_{60} molecules and inducing current flow through the dimer and further doubled by coupling to a third C_{60} . DFT-based calculations reveal that this trend is accompanied by an unprecedented increase in ZT of almost a factor of 16. Since S is an intensive property and is insensitive to the number of molecules conducting in parallel within a junction, we expect this increase to be manifest in self-assembled C_{60} -layers with two or more layers and this trend is expected to continue until the film thickness approaches the phase-breaking length of electrons. Since the tuning of intermolecular couplings is a generic strategy, our work points the way toward engineering thermopower enhancement in other organic species.

■ ASSOCIATED CONTENT

Supporting Information

Substrate preparation and experimental setup; building the experimental conductance histograms; thermal circuit; simultaneous measurement of thermopower and conductance during approach and retraction; computational methods; and building histograms from the theoretical calculations. This material is available free of charge via the Internet at <http://pubs.acs.org>.

■ AUTHOR INFORMATION

Corresponding Author

*E-mail (N.A.) nicolas.agrait@uam.es; (C.J.L.) c.lambert@lancaster.ac.uk.

Author Contributions

C.E. and K.G. contributed equally to this work.

Notes

The authors declare no competing financial interest.

■ ACKNOWLEDGMENTS

This work was supported by Spanish MICINN/MINECO through the programs MAT2011-25046 and CSD-2007-00010 *Nanociencia Molecular* (CONSOLIDER-INGENIO-2010), Comunidad de Madrid through program *Nanobiomagnet* S2009/MAT-1726, by the U.K. EPSRC and the European Union (FP7) through programs ITN "FUNMOLS" Project Number 212942, ITN NanoCTM and ELFOS. C.E. acknowledges funding from the A.G. Leventis Foundation.

■ REFERENCES

- (1) Malen, J. A.; Yee, S. K.; Majumdar, A.; Segalman, R. A. Fundamentals of energy transport, energy conversion, and thermal properties in organic–inorganic heterojunctions. *Chem. Phys. Lett.* **2010**, *491*, 109–122.
- (2) Reddy, P.; Jang, S.-Y.; Segalman, R. A.; Majumdar, A. Thermoelectricity in Molecular Junctions. *Science* **2007**, *315*, 1568.
- (3) Baheti, K.; Malen, J. A.; Doak, P.; Reddy, P.; Jang, S. Y.; Tilley, T. D.; Majumdar, A.; Segalman, R. A. Probing the Chemistry of Molecular Heterojunctions Using Thermoelectricity. *Nano Lett.* **2008**, *8*, 715–719.
- (4) Yee, S. K.; Malen, J. A.; Majumdar, A.; Segalman, R. Thermoelectricity in Fullerene Metal Heterojunctions. *Nano Lett.* **2011**, *11*, 4089.
- (5) Yee, S.; Malen, J.; Reddy, P.; Segalman, R.; Majumdar, A. *Thermoelectricity at the organic-inorganic interface*, Proceedings of the 14th International Heat Transfer Conference IHTC14, Washington, DC, August 7–13, 2010.
- (6) Malen, J. A.; Doak, P.; Baheti, K.; Tilley, T. D.; Majumdar, A.; Segalman, R. A. The Nature of Transport Variations in Molecular Heterojunction Electronics. *Nano Lett.* **2009**, *9*, 3406–3412.
- (7) Finch, C. M.; García-Suárez, V. M.; Lambert, C. J. Giant thermopower and figure of merit in single-molecule devices. *Phys. Rev. B* **2009**, *79*, 033405.
- (8) Widawsky, J. R.; Darancet, P.; Neaton, J. B.; Venkataraman, L. Simultaneous Determination of Conductance and Thermopower of Single Molecule Junctions. *Nano Lett.* **2012**, *12*, 354–358.
- (9) Schull, G.; Frederiksen, T.; Brandbyge, M.; Berndt, R. Passing Current through Touching Molecules. *Phys. Rev. Lett.* **2009**, *103*, 206803.
- (10) Rubio, G.; Agrait, N.; Vieira, S. Atomic-sized metallic contacts: mechanical properties and electronic transport. *Phys. Rev. Lett.* **1996**, *76*, 2302–5.
- (11) Leary, E.; González, M. T.; van der Pol, C.; Bryce, M. R.; Filippone, S.; Martin, N.; Rubio-Bollinger, G.; Agrait, N. Unambiguous One-Molecule Conductance Measurements under Ambient Conditions. *Nano Lett.* **2011**, *11*, 2236–2241.
- (12) Böhler, T.; Edtbauer, A.; Scheer, E. Conductance of individual C_{60} molecules measured with controllable gold electrode. *Phys. Rev. B* **2007**, *76*, 125432.
- (13) Kiguchi, M.; Murakoshi, K. Conductance of Single C_{60} Molecule Bridging Metal Electrodes. *J. Phys. Chem. C* **2008**, *112*, 8141–8143.
- (14) Néel, N.; Kröger, J.; Limot, L.; Frederiksen, T.; Brandbyge, M.; Berndt, R. Controlled Contact to a C_{60} Molecule. *Phys. Rev. Lett.* **2007**, *98*, 065502.
- (15) Dubi, Y.; Di Ventra, M. Heat flow and thermoelectricity in atomic and molecular junctions. *Rev. Mod. Phys.* **2011**, *83*, 131–155.
- (16) Rocha, A. R.; Garcia-Suarez, V.; Bailey, S. W.; Lamber, C. J.; Ferrer, J.; Sanvito, S. Spin and molecular electronics in atomically generated orbital landscapes. *Phys. Rev. B* **2006**, *73*, 085414.
- (17) Rocha, A. R.; Garcia-Suarez, V.; Bailey, S. W.; Lambert, C. J.; Ferrer, J.; Sanvito, S. Towards molecular spintronics. *Nat. Mater.* **2005**, *4*, 335–339.
- (18) Soler, J. M.; Artacho, E.; Gale, J. D.; García, A.; Junquera, J.; Ordejón, P.; Sánchez-Portal, D. The SIESTA method for ab initio order-N materials simulation. *J. Phys.: Condens. Matter* **2002**, *14*, 2745.